Effect of optical pumping on the momentum relaxation time of graphene in the terahertz range*

Zuo Zhi-Gao(左志高)[a)b)], Wang Ping(王 平)[a)b)], Ling Fu-Ri(凌福日)[b)†], Liu Jin-Song(刘劲松)[a)], and Yao Jian-Quan(姚建铨)[a)c)]

[a)] *Wuhan National Laboratory for Optoelectronics, Huazhong University of Science and Technology, Wuhan* 430074, *China*
[b)] *School of Optical and Electronic Information, Huazhong University of Science and Technology, Wuhan* 430074, *China*
[c)] *College of Precision Instrument and Opto-electronics Engineering, Tianjin University, Tianjin* 300072, *China*

(Received 13 November 2012; revised manuscript received 16 April 2013)

The momentum relaxation time of a photoexcited graphene in the THz frequency range has been studied by using terahertz time domain spectroscopy under optical pumping at room temperature. It is found that the momentum relaxation time of the graphene as a function of the optical pumping intensity exhibits a threshold behavior. The features of the momentum relaxation time as a function of the optical pumping intensity are also investigated. The results are useful for understanding the basic underlying physics of graphene scattering as well as finding the possible applications in carbon-based electronics.

Keywords: graphene, momentum relaxation time, optical pumping, terahertz

PACS: 73.50.Gr, 78.20.Ci **DOI:** 10.1088/1674-1056/22/9/097304

1. Introduction

Due to its remarkable properties, such as high mobility at room temperature, finite residual conductivity within the limit of vanishing carrier density, and the chiral quantum Hall effect,[1–5] graphene has become a focal point of experimental and theoretical researches over the past few years.[6–8] Recent experimental and theoretical studies have demonstrated that multilayer epitaxial graphene exhibits unusual electronic properties.[9–11] The unique properties of graphene[12,13] make it promising for various nanoelectronic device applications. Novel terahertz and infrared (IR) optoelectronic devices are proposed and evaluated, in particular, in Refs. [14]–[18]. Recent reports on the successful fabrication of ultrafast graphene transistors[19,20] and photodetectors[21,22] have further advanced this research frontier into the fields of electronics and optoelectronics. The graphene transistor was reported to be used both as an electrical modulator[23] with a frequency as high as $\sim$ 10 GHz and as a sensitive photo detector for imaging.[24]

The momentum relaxation time is one of the most fundamental quantities for the performance of semiconductor devices for controlling the charge transport, and the scattering is often described by this time constant. Photoconductance measurements are widely used to determine excess momentum relaxation time under illumination. At room temperature, the optical response of graphene in the THz frequency range is described by the free carrier response, which depends on both the total carrier concentration and the carrier distribution in energy.[14] Therefore, the THz response can be used to study the carrier relaxation dynamics in graphene.

In order to understand the dynamics of electrons and holes in graphene and the conduction mechanisms of graphene, in this work, we study the momentum relaxation time variation of photoexcited graphene in the THz frequency range under optical pumping in a wide range of intensities. Our results indicate that the obtained momentum relaxation time depends on the choice of the optical pumping intensity. The momentum relaxation time of the photoexcited graphene as a function of the optical pumping intensity is investigated as well.

2. Experiment

In our experiment we investigate a six-layer graphene sample supplied by the Advanced Chemicals Supplier, LLC of USA. The graphene is thermally grown on a 680-μm thick quartz substrate made by chemical vapor deposition (CVD), as reported elsewhere.[25]

We utilize a THz time domain spectrum (THz-TDS) system[26] produced by Zomega Terahertz Corporation of US to measure the transmittance spectrum at room temperature, as shown in Fig. 1. In this THz-TDS system, a fiber femtosecond laser beam (center wavelength of 780 nm, repetition rate of 50 MHz, pulse width of 90 fs) is divided into two beams

*Project supported by the National Natural Science Foundation of China (Grants Nos. 10974063 and 61177095), the Hubei Natural Science Foundation, China (Grant Nos. 2010CDA001 and 2012FFA074), the Research Foundation of Huazhong University of Science and Technology, China (Grant Nos. 01-09-230904 and 02-16-230008), the PhD Program Foundation of Ministry of Education of China (Grant No. 20100142110042), and the Fundamental Research Funds for the Central Universities, China (Grant Nos. HUST: 2010MS041 and 2011TS001).

†Corresponding author. E-mail: lingfuri@163.com

© 2013 Chinese Physical Society and IOP Publishing Ltd

(pump and probe beams) by a polarized beam splitter PBS1. A half-wave plate (HWP) is placed to change the ratio between the pump and the probe beams. The pump beam is reflected by retro-reflector RR1. After passing twice through QWP1 oriented at 45°, it is reflected by PBS1, and focused through lens L1 on a GaAs emitter to generate the THz radiation. The probe beam is directed to the polarized beam splitter PBS2 by mirrors M1 and M2. The reflected beam passes through the quarter wave plate QWP2, and is reflected by retro-reflector RR2 and mirror M3. The RR1 and RR2 are attached together on a linear step stage to form a time delay line. After two passes through PBS2, the probe beam is directed to a ZnTe crystal and a balance detector BD through mirrors M4 and M5, lens L2, and an ITO crystal. Meanwhile, the generated THz radiation is collimated by an off-axis parabolic mirror OAP1, and passes through two confocal polyethylene lenses L3 and L4. The sample is placed at the focus of L3 and L4. At last, the transmitted THz radiation is focused by off-axis parabolic mirror OAP2 and reflected by the ITO crystal to the ZnTe crystal and BD for coherent detection. The detectable frequency range is from 0.1 THz to 1 THz (3.3–33.3 cm^{-1}) with a dynamic range of more than 60 dB. The measured frequency resolution is 10 GHz, and the spot size at the focus is 3 mm. An all-solid-state YAG laser (center wavelength of 1064 nm) is employed in the experiment to provide the external optical pump. The light is obliquely incident upon the surface of the sample at an angle of 45° with the graphene sample surface, and the spot size is 5 mm in diameter.

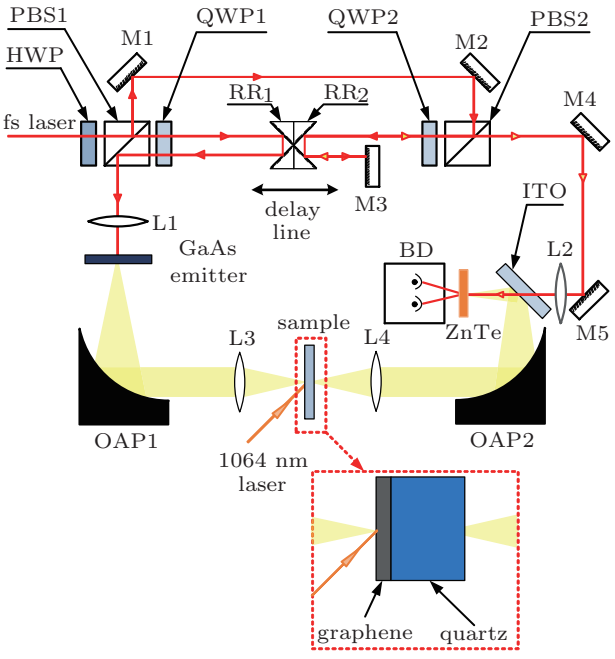


Fig. 1. (color online) Schematic diagram of THz-TDS. An all-solid-state YAG laser illuminates the surface of the sample at an angle of 45° to the THz beam axis.

3. Results and discussion

Figure 2 shows the time domain waveforms of the sample at room temperature. The time delay between the reference and the sample signal with no external optical illumination is approximately 1.8 ps. When the YAG laser is employed to illuminate the graphene as described above, we can observe small time delay and amplitude decreases as the external optical intensity increases, as shown in Fig. 2(b).

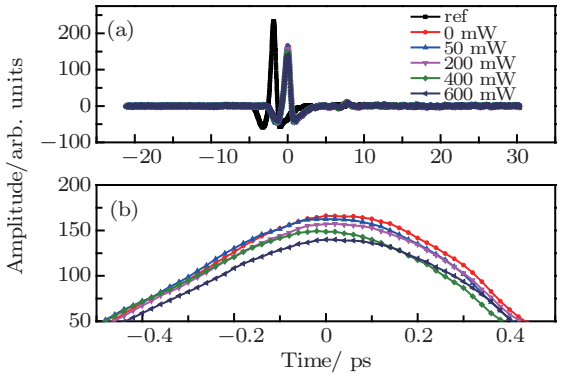


Fig. 2. (color online) (a) Time domain waveforms of the sample of six-layer graphene grown on quartz and (b) time delay and amplitude decreases under different intensities of external optical illumination.

The transmittance spectra of the quartz and the graphene on the quartz substrate are obtained, as shown in Figs. 3(a) and 3(b). The transmittance spectrum of graphene is given as $T_G = T_{G_Quartz}/T_{Quartz}$, where T_G, T_{G_Quartz}, and T_{Quartz} represent the transmittances of graphene, graphene on quartz substrate, and quartz wafer, respectively. It is clearly found that the graphene's transmittance in the THz range decreases with increasing pumping intensity. The reason is that the photogenerated electron density in the conduction band increases with increasing pumping intensity and causes the transmittance in the THz range to decrease, owing to the effect of the Drude absorption.

Matching the optical boundary conditions at the air/graphene/quartz interfaces, the steady-state conductivities with different pumping intensities can be calculated from the THz transmittance spectra. The complex amplitude transmittance T in the THz range through the graphene on a quartz wafer (normalized to the transmission through a plain quartz wafer) can be written in terms of the complex optical conductivity as[27]

$$T(\omega) = \left|1 + N\sigma(\omega)\sqrt{\mu_0/\varepsilon_0}/(1+n_{quartz})\right|^{-2}, \qquad (1)$$

where T is the transmittance of graphene, N is the number of graphene layers, σ is the steady-state photo-generated conductivity, μ_0 and ε_0 are the permeability and the dielectric constant of the free space, respectively, and n_{quartz} is the refractive index of the quartz wafer. The frequency dependence of the steady-state conductivity of graphene under different external

optical pumping intensities are obtained, as shown by the dotted lines in Fig. 4.

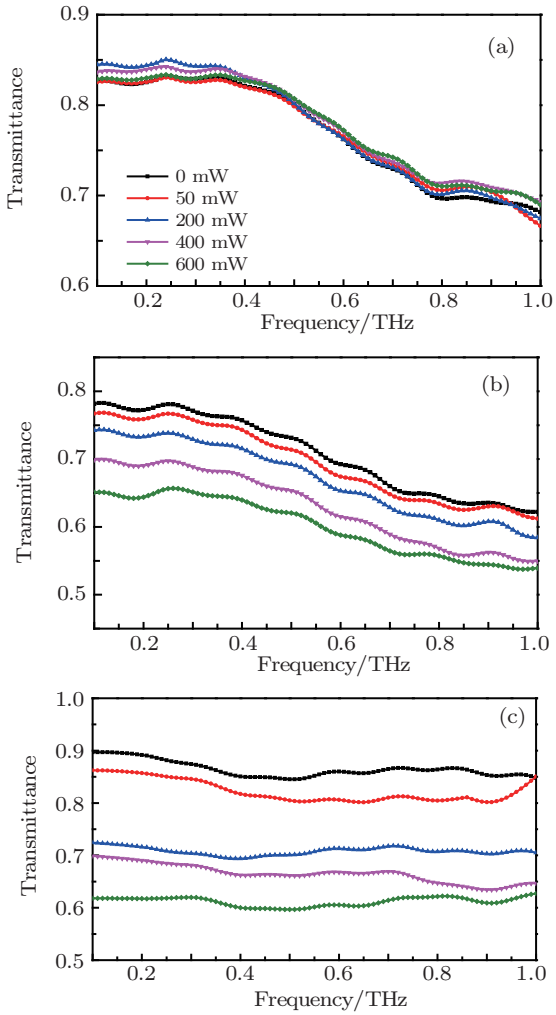


Fig. 3. (color online) Transmittance spectra of (a) quartz wafer, (b) graphene on quartz substrate, and (c) graphene in the THz frequency range.

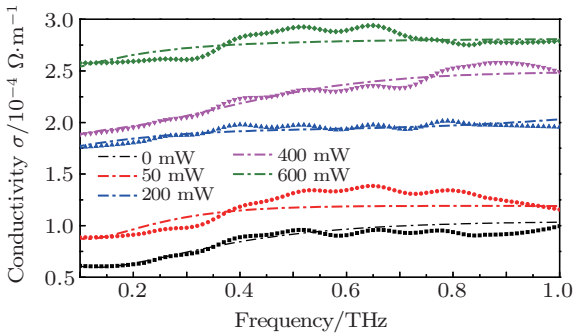


Fig. 4. (color online) Measured steady-state conductivity of six-layer graphene under different external optical pumping obtained using Eq. (1) (dot lines), along with the theoretical simulated results (dash lines).

It has been reported that the studies of photoconduction in graphene can be used for revealing the mechanism of free carrier relaxation process.[28] In order to illustrate the micromechanisms responsible for the relaxation dynamics in the photoexcited graphene clearly, it is worthwhile to study the momentum relaxation time as a function of the pumping intensity.

According to Ref. [29], the real part of the ac conductivity comprises the contributions of both interband and intraband transitions accompanied by the absorption and emission of photons

$$\mathrm{Re}\,\sigma_\omega = \mathrm{Re}\,\sigma_\omega^{\mathrm{inter}} + \mathrm{Re}\,\sigma_\omega^{\mathrm{intra}}. \tag{2}$$

Here the contributions of interband and intraband transitions[30] to the ac conductivity are given respectively as

$$\mathrm{Re}\,\sigma_\omega^{\mathrm{inter}} = \frac{e^2}{4\hbar}\tanh\left(\frac{\hbar\omega - 2\varepsilon_{\mathrm{F}}}{4k_{\mathrm{B}}T}\right), \tag{3}$$

$$\mathrm{Re}\,\sigma_\omega^{\mathrm{intra}} = \frac{2\ln 2}{\pi\hbar^2}\frac{e^2\tau k_{\mathrm{B}}T}{(\omega\tau)^2+1}, \tag{4}$$

where the electron charge $e = 1.602\times10^{-19}$ C, the Boltzmann constant $k_{\mathrm{B}} = 1.381\times10^{-23}$ J/K, $T = 300$ K, $\hbar = 1.055\times10^{-34}$ J·s. The Fermi energy is proportional to the intensity of the external optical pumping I_{pump}, $\varepsilon_{\mathrm{F}} \propto I_{\mathrm{pump}}$.[29]

With the measured conductivity data and Eqs. (2)–(4), we use the curve fitting method to obtain the momentum relaxation time τ. The dashed lines in Fig. 4 represent the curve fitting results. The carrier momentum relaxation time has a magnitude of 0.2–4.5 ps, as shown in Fig. 5(a).

In general, the relaxation dynamics in graphene is expected to have density dependencies on the carrier density,[18,28,29] and the momentum relaxation time is inversely proportional to the carrier density[31]

$$\tau_{\mathrm{p}} \propto \frac{1}{n} \propto \frac{1}{N_0 + bP_{\mathrm{pump}}}, \tag{5}$$

where n is the carrier density, which is proportional to the external optical pump power P_{pump}, N_0 is the total carrier number in graphene without external optical pumping, and bP_{pump} represents the photoexcited carrier number. The solid line in Fig. 5(a) shows the fitting result by using Eq. (5) and the experimental results.

From Fig. 5(a), it can be found that the momentum relaxation time as a function of the pumping intensity exhibits a threshold behavior with a rapid decrease at low pumping intensities and a slow decrease with strong pump. Here the threshold value is defined as the external optical pump intensity at 1/e of the maximum momentum relaxation time. In Fig. 5(a), the threshold value of the six-layer graphene is 46 mW. For a pumping intensity less than this threshold value, an increase in pumping intensity leads to an increase in the photogeneration of electrons in the conduction band and holes in the valence band, and this decreases the momentum relaxation time rapidly, which is consistent with the theoretical prediction in Ref. [18]. However, when the pumping intensity is larger than this threshold value, the relaxation time decreases slowly with

increasing pumping intensity. The necessary process might be that a strong pumping intensity would generate larger carrier densities and this could make the Coulomb interaction less effective due to the effect of carrier density screening. As a result, the relaxation time is less sensitive to the pumping intensity.

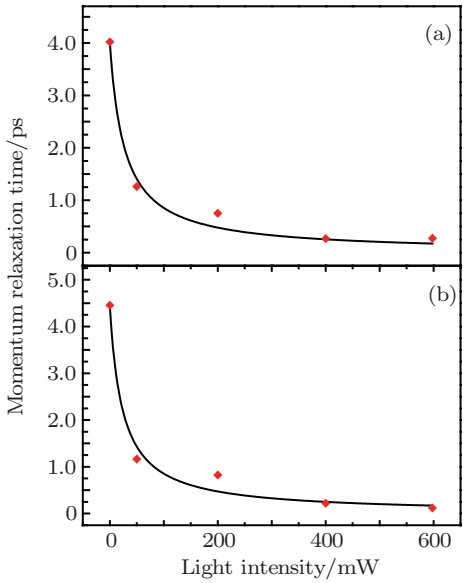


Fig. 5. (color online) Light intensity dependence of momentum relaxation time (dot line) and fitting result (solid line). The results of (a) six-layer and (b) monolayer graphene samples are shown.

In order to illuminate the effect of different numbers of layers on the carrier momentum relaxation time of graphene, we also study the light intensity dependence of momentum relaxation time for a monolayer graphene sample, which is supplied by Advanced Chemicals Supplier, LLC of USA as well, with the same method, as shown in Fig. 5(b). Comparing this with Fig. 5(a), it can be found that the moment relaxation time of the monolayer graphene behaves like the six-layer sample, and the threshold value is 40 mW, which is smaller than that of the six-layer sample. This difference can be explained by the fact that, according to Eq. (5), the concentration of photo-induced carriers in the monolayer graphene is higher than that in the six-layer graphene under the same external optical pumping intensity. Due to the carrier density screening, the relaxation time of monolayer would be less effective to the external optical pump intensity. As a result, as the optical pump intensity increases, the monolayer graphene sample reaches the threshold value more quickly than the six-layer graphene sample.

4. Conclusion

We have measured the carrier momentum relaxation time of graphene by using terahertz time domain spectroscopy under optical pumping at room temperature. Results show that when the intensity of the pumping electric field is less than a threshold value, the carrier momentum relaxation time decreases rapidly with increasing pumping intensity. When the intensity of the pumping electric field is larger than the threshold value, the carrier momentum relaxation time decreases slowly. The behavior of the carrier momentum relaxation time with optical pumping intensity is explained according to the electron–phonon interaction in graphene. The results of the current research are expected to be very useful for understanding and designing high-power and high-speed graphene emitters and detectors in the terahertz frequency range.

References

[1] Novoselov K S, Geim A K, Morozov S V, Jiang D, Zhang Y, Dubonos S V, Grigorieva I V and Firsov A A 2004 *Science* **306** 666
[2] Novoselov K S, Geim A K, Morozov S V, Jiang D, Zhang Y, Dubonos S V, Grigorieva I V and Firsov A A 2005 *Nature* **438** 197
[3] Castro Neto A H, Guinea F, Peres N M R, Novoselov K S and Geim A K 2009 *Rev. Mod. Phys.* **81** 109
[4] Morozov S V, Novoselov K S, Katsnelson M I, Schedin F, C.Elias D, Jaszczak J A and Geim A K 2008 *Phys. Rev. Lett.* **100** 016602
[5] Novoselov K S, Jiang Z, Zhang Y, Morozov S V, Stormer H L, Zeitler U, Maan J C, Boebinger G S, Kim P and Geim A K 2007 *Science* **315** 1379
[6] Pan Y, Shi D X and Gao H J 2007 *Chin. Phys.* **16** 3151
[7] Tang C, Ji L, Meng L J, Sun L Z, Zhang K W and Zhong J X 2009 *Acta Phys. Sin.* **58** 7815 (in Chinese)
[8] Han P Y, Liu W, Xie Y H and Zhang X C 2009 *Physics* **38** 395
[9] Choi H Y, Borondics F and Siegel D A 2009 *IEEE* **978**
[10] Novoselov K S, Geim A K, Morozov S V, Jiang D, Katsnelson M I, Grigorieva I V, Dubonos S V and Firsov A A 2005 *Nature* **438** 197
[11] Geim A K and Novoselov K S 2007 *Nat. Mater.* **6** 183
[12] Castro Neto A H, Guinea F, Peres N M R, Novoselov K S and Geim A K 2009 *Rev. Mod. Phys.* **81** 109
[13] Vasko F T and Ryzhii V 2008 *Phys. Rev. B* **77** 195433
[14] Berger C, Song Z, Li T, Li X, Ogbazhi A Y, Feng R, Dai Z, Marchenkov A N, Conrad E H, First P N and Heer W A 2004 *J. Phys. Chem. B* **108** 19912
[15] Rana F 2008 *IEEE Trans. Nanotechnol.* **7** 91
[16] Dubinov A A, Aleshkin V Ya, Ryzhii M, Otsuji T and Ryzhii V 2009 *Appl. Phys. Express* **2** 092301
[17] Ryzhii V, Mitin V, Ryzhii M, Ryabova N and Otsuji T 2008 *Appl. Phys. Express* **1** 063002
[18] Ryzhii V and Ryzhii M 2009 *Phys. Rev. B* **79** 245311
[19] Lin Y M, Dimitrakopoulos C, Jenkins K A, Farmer D B, Chiu H Y, Grill A and Avouris P 2010 *Science* **327** 662
[20] Zhao J, Zhang G Y and Shi D X 2013 *Chin. Phys. B* **22** 057701
[21] Mueller T, Xia F and Avouris P 2010 *Nat. Photonics* **4** 297
[22] Lu M, Yuan J, Wen B, Liu J, Cao W Q and Cao M S 2013 *Chin. Phys. B* **22** 037701
[23] Lin Y M, Jenkins K A, Valdes-Garcia A, Small J P, Farmer D B and Avouris P 2009 *Nano Lett.* **9** 422
[24] Xia F, Mueller T, Golizadeh M R, Freitag M, Lin Y M, Tsang J, Perebeinos V and Avouris P 2009 *Nano Lett.* **9** 1039
[25] Novoselov K S, Jiang D, Schedin F, Booth T J, Khotkevich V V, Morozov S V and Geim A K 2005 *Proc. Natl. Acad. Sci. USA* **102** 10451
[26] Brian S 2008 *Miniature Terahertz Time-domain Spectrometry* (Ph.D. dissertation) (New York: Rensselaer Polytechnic Institute)
[27] Dawlaty J M, Shivaraman S, StraitJ, George P, Chandrashekhar M, Rana F, Spencer M G, Veksler D and Chen Y Q 2008 *Appl. Phys. Lett.* **93** 131905
[28] Satou A, Vasko F T and Ryzhii V 2008 *Phys. Rev. B* **78** 115431
[29] Ryzhii V, Ryzhii M and Otsuji T 2007 *J. Appl. Phys.* **101** 083114
[30] Mak K F, Sfeir M Y, Wu Y, Lui C H, Misewich J A and Heinz T F 2008 *Phys. Rev. Lett.* **101** 196405
[31] Zhang H C, Deng L, Wen J H, Liao R, Lai T S and Lin W Z 2001 *Science in China Ser. A* **44** 1340